Cell, Vol. 97, 805–815, June 11, 1999, Copyright ©1999 by Cell Press

A Structural Explanation for the Binding of Multiple Ligands by the α-Adaptin Appendage Domain

David J. Owen,* Yvonne Vallis,* Martin E. M. Noble,† Jack B. Hunter,* Tim R. Dafforn,‡ Philip R. Evans,*§ and Harvey T. McMahon*§

*MRC Laboratory of Molecular Biology
Hills Road
Cambridge CB2 2QH
United Kingdom
†Laboratory of Molecular Biophysics
Oxford University
South Parks Road
Oxford OX1 3QU
United Kingdom
‡Structural Medicine
Department of Haematology
CIMR
University of Cambridge
Hills Road
Cambridge CB2 2XY
United Kingdom

Summary

The α subunit of the endocytotic AP2 adaptor complex contains a 30 kDa "appendage" domain, which is joined to the rest of the protein via a flexible linker. The 1.9 Å resolution crystal structure of this domain reveals a single binding site for its ligands, which include amphiphysin, Eps15, and epsin. This domain when overexpressed in COS7 fibroblasts is shown to inhibit transferrin uptake, whereas mutants in which interactions with its binding partners are abolished do not. DPF/W motifs present in appendage domain–binding partners are shown to play a crucial role in their interactions with the domain. A single site for binding multiple ligands would allow for temporal and spatial regulation in the recruitment of components of the endocytic machinery.

Introduction

In 1964 ultrastructural studies on mosquito oocytes described yolk protein internalization through coated pits on the cell surface into coated vesicles (Roth and Porter, 1964). The process by which these specialized areas of the plasma membrane are internalized, and the subsequent targeting of these vesicles to multiple destinations throughout the cell, have been extensively studied (for reviews, see DeCamilli and Takei, 1996; Schekman and Orci, 1996; Robinson, 1997; Schmid, 1997). The major components of the coats, purified from coated vesicles, were identified as clathrin triskelia and adaptor protein complexes (APs) (Pearse, 1976; Keen, 1987; for review, see Pearse and Robinson, 1990). The AP complex found at the plasma membrane, AP2, was shown to bind and cluster transmembrane proteins destined for internalization and to promote clathrin polymerization. The formation of a cage structure from clathrin helps to invaginate the membrane, and the scission of the nascent vesicle is achieved with the aid of the GTPase dynamin (Schmid et al., 1998). This clathrin-mediated pathway for endocytosis is involved in many functions, including downregulation of signaling for growth factor receptors, the uptake of nutrients bound to their appropriate receptors, and the maintenance of membrane identity, as in neurons where it retrieves synaptic vesicle proteins after exocytosis. Some forms of cancer have been linked to gene fusions of proteins implicated in endocytosis (Floyd and DeCamilli, 1998), and some viruses gain access to the intracellular milieu by "hijacking" the pathway (DeTulleo and Kirchhausen, 1998; Oldridge and Marsh, 1998).

Clathrin/clathrin adaptor–mediated pathways of vesicle budding occur not only at the plasma membrane but also at the Golgi and endosome membranes. The adaptors used on intracellular membrane compartments, AP1, AP3, and AP4, have the same gross structure but utilize homologous subunits to provide the differential specificity for cargo and regulatory molecules (Robinson, 1997; Odorizzi et al., 1998). In trafficking between the endoplasmic reticulum and the Golgi, a different coat/adaptor system, the COPs, is used (Kreis et al., 1995; Schekman and Orci, 1996). At the plasma membrane, clathrin-mediated endocytosis occurs alongside other non–clathrin-mediated pathways such as phagocytosis, macropinocytosis, and caveoli formation, the mechanisms of which are poorly understood (Swanson and Watts, 1995; Anderson, 1998).

All AP complexes comprise four types of subunit: two large (~110 kDa) (α and β2 in AP2), one medium (~50 kDa) (μ2 in AP2), and one small (~17 kDa) (σ2 in AP2). Deep-etch electron microscopy of adaptors shows them to have a "brick"-shaped central core or "trunk" domain connected via flexible linkers to two appendage domains, also called "ears" (Heuser and Keen, 1988). In these images the adaptors appear to interact with clathrin via their appendage domains, and only in the presence of these appendages do they promote clathrin self-assembly (Zaremba and Keen, 1985; Heuser and Keen, 1988). The appendage domains correspond to the C-terminal 25–30 kDa portions of the α- and β-adaptin 100 kDa chains. When the ears have been proteolytically cleaved from adaptors, the brick-shaped portion, which contains the remainder of α and β as well as the μ2 and σ2 subunits, can still bind to membranes containing proteins to be internalized (Peeler et al., 1993). The μ2 subunit is the part of the complex that binds to Yxxø motifs (where ø is a hydrophobic residue) on cytoplasmic portions of proteins to be internalized and thus defines what is internalized by the pathway (Ohno et al., 1995; Owen and Evans, 1998). Thus, in clathrin-coated vesicles there is an outer protein shell of polymerized clathrin triskelia making a lattice of hexagons and pentagons, a middle layer where clathrin and the appendage domains of the adaptor meet, and an

§To whom correspondence should be addressed (e-mail: hmm@mrc-lmb.cam.ac.uk [H. T. M.], pre@mrc-lmb.cam.ac.uk [P. R. E.]).

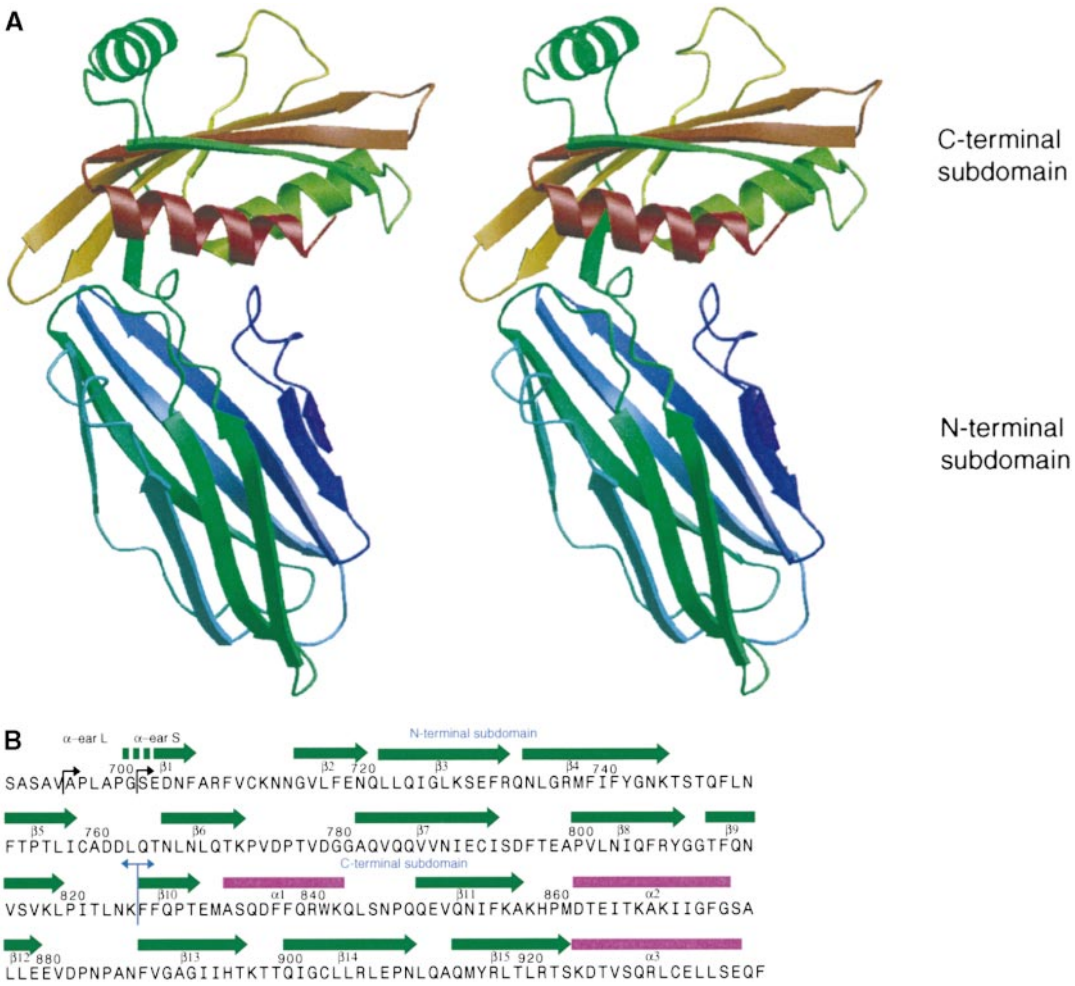

Figure 1. Structure of α-Adaptin Appendage Domain

(A) Stereo view of the appendage domain, colored from blue (N terminus) to red (C terminus), showing the N-terminal β sandwich subdomain and the mixed C-terminal subdomain.

(B) Sequence of the appendage domain of α-adaptin indicating the positions of β strands (green), α helices (magenta), and subdomain boundaries.

inner layer made of the main body of adaptors associated with the membrane (Smith et al., 1998).

The β subunit of clathrin adaptors promotes clathrin coat assembly (Gallusser and Kirchhausen, 1993), with direct binding to clathrin being located at the linker between the trunk and the appendage domain (Shih et al., 1995). Recent studies have identified several proteins that may bind to the α-adaptin appendage domain, including dynamin (Wang et al., 1995), amphiphysin heterodimers (Wang et al., 1995; David et al., 1996; Wigge et al., 1997a, 1997b), Eps15 (Benmerah et al., 1995; Tebar et al., 1996), and epsin (Chen et al., 1998). In order to investigate further the role of the α-adaptin appendage domain in endocytosis, we have solved its structure to 1.9 Å resolution by X-ray crystallography. The structure allowed us to improve the definition of the appendage domain boundary and, as a result, produce a protein with increased solubility for use in in vitro experiments and that was capable of inhibiting clathrin-mediated endocytosis in vivo. An analysis of the protein's molecular surface identified a single candidate binding site for the amphiphysins, Eps15, and epsin. This identification was confirmed using both in vitro binding assays and in vivo endocytosis assays on point mutants designed on the basis of the structure. Data are presented to show that the sequence motif DPF/W, present in all appendage domain ligands, plays a central role in these interactions. The implications for the role of this domain of the adaptor complex in the recruitment of multiple ligands and in the formation of clathrin-coated vesicles are discussed.

The Structure

The 1.9 Å resolution crystal structure of the appendage domain of α-adaptin (termed α-ear$_S$) was solved by isomorphous replacement (see Experimental Procedures). The structure can be divided into two subdomains (Figure 1). The N-terminal subdomain, comprising residues S701–K824, is a nine-stranded β sandwich, which is reminiscent of an immunoglobulin fold. The C-terminal subdomain (residues F825–F938) is made up of a five-stranded β sheet (one of which is interrupted) flanked by helix α1 on one face and by two helices (α2 and α3) on

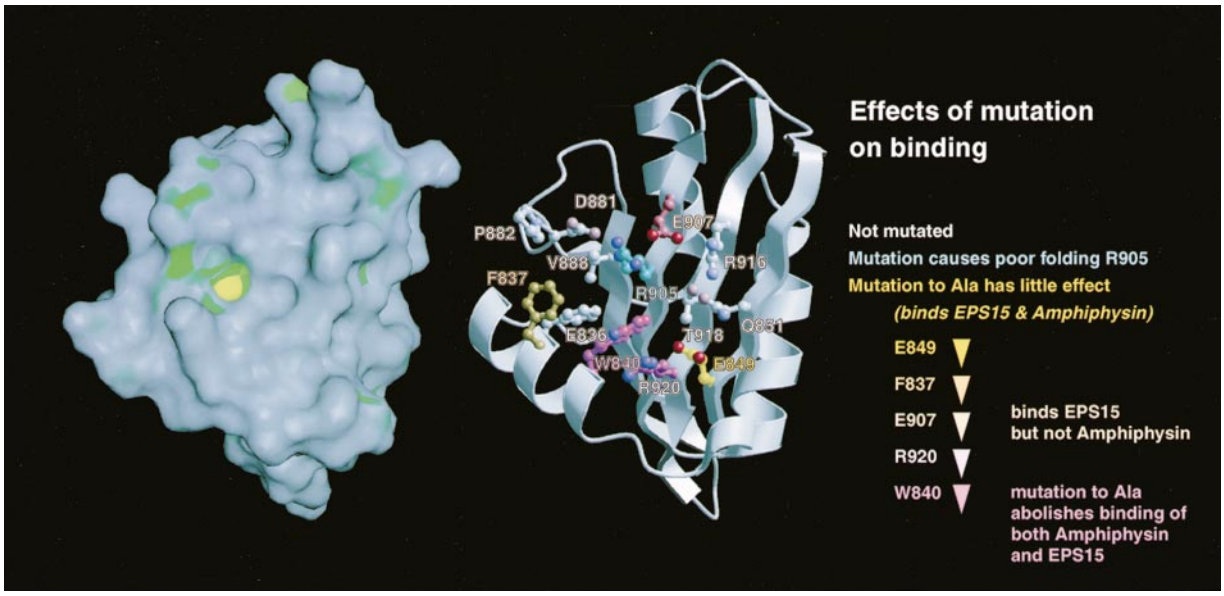

Figure 2. Top Views of the C-Terminal Subdomain

(Left) Surface colored such that the sites of favorable hydrophobic interaction are colored yellow, sites of moderate hydrophobic interaction are colored green, and sites of neutral or disfavored hydrophobic interaction are colored gray. The outstanding feature (strongly yellow) is the hydrophobic pocket caused by W840.

(Right) Positions of point mutants and other residues around W840. Mutation of this residue abolishes the α-adaptin ear interaction with its binding partners. Mutations in residues surrounding W840 cause varying degrees of inhibition of ligand binding as indicated by color: yellow (no effect) through orange and pink (partial effect) to purple (abolition of ligand binding).

the other. This subdomain bears no obvious structural relationship to any previously known domain. The subdomains are joined by a short linker, and the resulting interface contains tightly packed and mostly hydrophobic residues, suggesting that the relative subdomain orientation is fixed (accessible surface buried 1430 Å^2). The compact nature of this interface also explains the lack of protease sensitivity between the subdomains (data not shown). This is the domain released by elastase treatment of adaptors and has been used previously (Wang et al., 1995). The structure showed that in the construct used (residues 701–938) the protein was truncated in the center of a β strand (strand 1), providing an explanation for the low yield of correctly folded and therefore soluble protein (see Experimental Procedures). A new longer construct comprising residues 695–938, termed α-ear$_L$, in which the N terminus was elongated by six residues to complete the β strand, resulted in a protein with higher solubility. This construct was used in all subsequent studies.

Locating the Binding Site

Protein–protein interactions require both an appropriate affinity and a high level of specificity. This is achieved by a mixture of polar (hydrogen bonding/electrostatic) and apolar (van der Waal's, hydrophobic) contacts, often found as a hydrophobic contact surface surrounded by a complementary series of polar groups. Much of the favorable energy of interaction arises from the displacement of water molecules when two hydrophobic surfaces match. Polar interactions are generally not very different in energy to the interactions with water that they replace, so polar interactions contribute more to specificity than to affinity. It should be possible to identify likely sites for protein–protein interactions by scanning a protein surface for regions of favorable hydrophobic contact. The apolar surface of a protein can be characterized by evaluating at each position on the surface the summed pairwise interactions of a hydrophobic probe in contact with the surface, if it is considered to displace a water from that position. The appropriate pairwise potential is favorable where van der Waal's interactions may be formed but is disfavored by the availability of hydrogen bonding atoms. Such a hydrophobic potential function has been implemented in the program GRID (Goodford, 1996).

Hydrophobic surface potential analysis of the entire α-adaptin appendage domain revealed a single candidate protein-binding site centered around W840 and potentially also containing F837, E849, R905, E907, and R920 (Figure 2). In order to test the validity of this hypothesis, alanine mutants were created in each of these residues for in vitro (as GST fusion constructs) and in vivo studies (as Myc-tagged fusion constructs).

The fold of each mutant was checked by circular dichroism (CD) measurements on the appendage domain cleaved from the GST fusion protein (Table 1). The mutants F837A, E849A, and E907A had identical CD spectra to that of α-ear$_L$. W840A and R920A, while having identical shaped CD spectra to wild-type α-ear$_L$, showed a very slight reduction in secondary structure content (less than a 4% reduction in molar ellipticity), indicating that these mutations may have caused very limited local unfolding. This is not surprising given the tight packing of these side chains as indicated by their good electron density in the wild-type structure. The R905A mutation

Table 1. α-Adaptin Appendage Domain Constructs

α-Adaptin Appendage Domain Construct	Folded/Soluble	Amphiphysin Binding	Eps15 Binding	Epsin Binding	Auxilin Binding	AP180 Binding	Cells Blocked for Endocytosis (%)
α-ear$_S$	Low	+	+	+	+	+	Insoluble
α-ear$_L$	Yes	++++	++++	++++	++++	++++	63 ± 1
N-terminal subdomain	Low	—	—	—	—	—	NA
C-terminal subdomain	No	—	—	—	—	—	NA
α-ear-50	No	—	—	—	—	—	NA
R707S	Yes	++++	++++	++++	++++	++++	65
F837A	Yes	+	++	++++	+++	—	ND
W840A	Yes	—	—	—	—	—	0 ± 1
E849A	Yes	+++	+++	++++	+++	++	33 ± 3
R905A	No	—	—	+	—	—	Insoluble
E907A	Yes	—	++	+++	+	—	25 ± 5
R920A	Yes	—	+	+++	+	—	0 ± 4

The table summarizes the data obtained on constructs used in this paper. α-ear$_S$ (residues 701–938); α-ear$_L$ (residues 695–938); N-terminal subdomain (residues 695–829); C-terminal subdomain (residues 824–938); α-ear-50 (residues 754–938). Number of plus signs indicates strength of binding. NA, not applicable; ND, not determined.

displayed a marked reduction in secondary structure and gave very low yields after cleavage, indicating that the C-terminal domain was unfolded causing the protein to become largely insoluble.

In vitro binding studies of α-ear$_L$ mutants show the residues important for interactions with ligands (Figure 3 and summary of all constructs in Table 1). Studies initially concentrated on the interactions of amphiphysin, Eps15, and epsin, but other potential binding partners of α-adaptin appendage domain (which are discussed later) have also been immunoblotted. The mutants show qualitatively similar effects on amphiphysin and Eps15 binding, but the amphiphysin interaction is more easily disrupted (see E907A and R920A), implying a weaker binding. These data indicate that a single binding site on the α-adaptin appendage domain exists for all these proteins, on the C-terminal subdomain. The binding of epsin is different to that of the other proteins in that although its binding is still strongly inhibited by mutating W840, there is only a weak effect on binding as a result of mutations in E907 and R920. This may be caused by the DPW motif of epsin binding in a slightly different manner to the DPF motif present on the other ligands or by epsin having the highest affinity of all the α-adaptin ligands tested.

Constructs lacking 50 residues at the N terminus (corresponding to the first three β sheet strands) have been used in several studies (Benmerah et al., 1996; Chen et al., 1998) that have suggested the involvement of the N terminus of the α-adaptin appendage domain in Eps15 and epsin recruitment. We have made this deletion construct and also a point mutant within this deletion at R707, which is located on the edge of β strand 1. Constructs encoding the individual subdomains were also made. The R707S mutant showed an identical CD spectra and ligand binding to wild-type α-ear$_L$. The N-terminal β sandwich subdomain, which had low solubility, showed no binding to any of the endocytosis proteins tested, and both the C-terminal subdomain and the construct lacking 50 N-terminal residues were completely insoluble and were thus unable to form any interactions (see Table 1). The low solubility of these constructs is probably caused by aggregation due to exposure to solvent of hydrophobic residues that participate in the subdomain interface or in the hydrophobic core of the subdomain. No function can be currently assigned to the N-terminal β sandwich subdomain, and it may thus function as a scaffolding domain that displays the C-terminal subdomain in the correct manner away from the "trunk" domain of the adaptor complex.

α-Adaptin Appendage Domain Blocks Endocytosis

In order to investigate the effect of the α-adaptin appendage domain on clathrin-mediated endocytosis, α-ear$_L$, fused to an N-terminal Myc tag, was transfected into COS cells under the control of a CMV promoter. Transferrin endocytosis was assayed as shown in Figure 4. The results (summarized in bar graph and Table 1) show that the overexpression of α-ear$_L$ resulted in a significant inhibition of transferrin uptake (63% ± 1% of cells inhibited by more than 80%). The effects of mutant forms of α-ear$_L$, W840A, E849A, R905A, E907A,

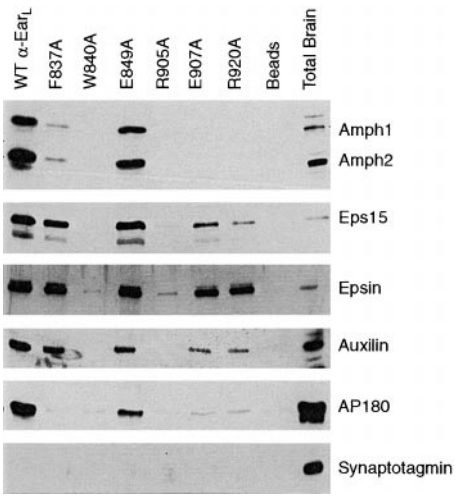

Figure 3. Mapping the Binding Site by Point Mutagenesis

GST-α-adaptin ear$_L$ point mutants tested for their ability to bind proteins in pull-down experiments from brain cytosol detected by immunoblotting. Synaptotagmin, an abundant protein in brain, is used as a control to show that binding is specific. Amph, amphiphysin.

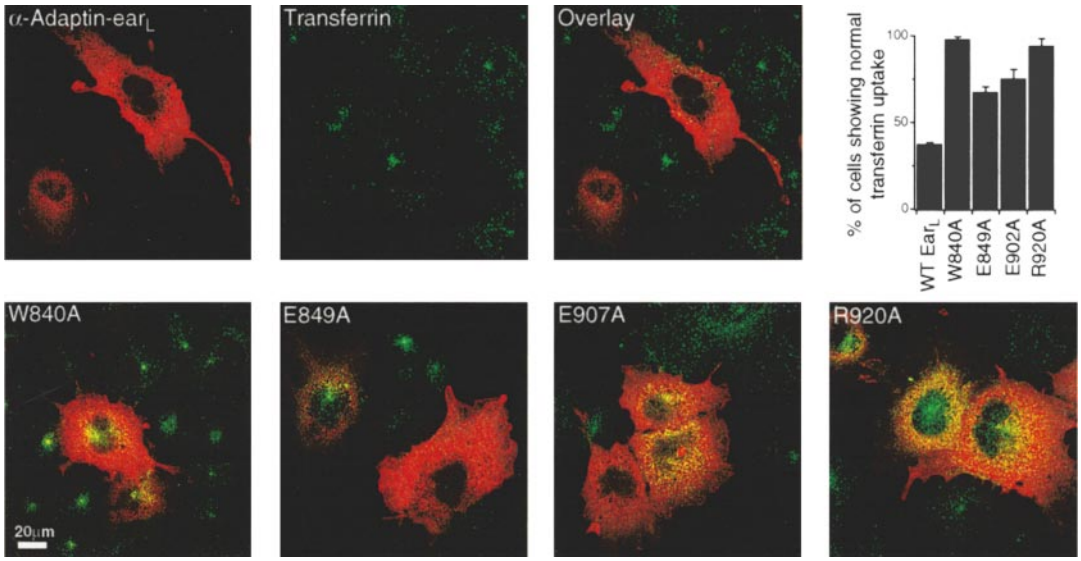

Figure 4. Effects of Wild-Type α-Adaptin Appendage Domain and Point Mutants on Transferrin Uptake in COS Cells

Immunofluorescence data of transferrin uptake (green) in cells transiently transfected with the α-ear$_L$ domain (stained red). In over 60% of cells the wild-type appendage domain inhibits transferrin uptake by >80% (top panels, lack of green perinuclear staining). The point mutants that are defective in ligand binding (see Figure 3) are accordingly less effective at causing inhibition of endocytosis (overlay images in bottom panel). Results are summarized in the bar chart for >100 transfected cells ± SEM. Bar, 20 μm.

and R920A were also investigated. The results mirrored those of the in vitro binding experiments showing that the mutants unable to bind either Eps15 or amphiphysin (W840A and R920A) did not affect transferrin uptake. The two glutamate mutants that showed attenuated Eps15 and amphiphysin binding resulted in 25% ± 5% (E907A) and 33% ± 3% (E849A) of cells blocked in transferrin uptake. The mutant R905A was completely insoluble when expressed in COS cells, so data for this construct has been omitted.

α-Adaptin-Binding Partners

The domain of Eps15 that interacts with the α-adaptin appendage domain has been mapped to the C-terminal third of the protein (Benmerah et al., 1996; Iannolo et al., 1997), where a major feature is the presence of 13 interspersed repeats of the sequence DPF. Although deletion analysis concluded that the DPF motif was not critical for the interaction with α-adaptin, binding was progressively reduced by successive truncations of the domain, which deleted increasing numbers of the DPF motifs (Iannolo et al., 1997). The presence of DPF motifs is also the major conserved feature between the adaptin-binding domain of Eps15 and the related Eps15R (Carbone et al., 1997). The N-terminal domain of amphiphysin that binds to the α-adaptin appendage domain (Wang et al., 1995; David et al., 1996; Wigge et al., 1997b; Slepnev et al., 1998) also contains a single DPF motif, although it has not been suggested to play a role in the interaction. Epsin, which has also been shown to bind to the α-adaptin appendage domain (Chen et al., 1998), contains nine copies of the related sequence motif DPW. If the DPF/W motif plays a role in mediating binding to α-adaptin, then it should be possible to identify other ligands of the appendage domain by virtue of the presence of the motif. Searches of proteins involved in endocytosis showed that other proteins contain DPF/W motifs. AP180, a protein that binds to clathrin and is involved in promoting clathrin cage assembly and regulating vesicle size (Ahle and Ungewickell, 1986; Ye and Lafer, 1995; Zhang et al., 1998; for review, see McMahon, 1999), contains two DPF sequences. Auxilin (Lindner and Ungewickell, 1992), a protein involved in clathrin cage disassembly, contains three DPF motifs, and the light chain of clathrin has one.

These DPF/W motif–containing proteins can be detected in GST α-ear$_L$ pull-down experiments from brain cytosol (Figures 3 and 6A), and in the converse experiment α-adaptin can be detected in pull-down experiments with GST fusion proteins of the DPF/W domains of amphiphysin, Eps15, epsin, and full-length AP180 (Figure 5A). In order to establish the direct interaction between these proteins and the α-adaptin appendage domain, α-ear$_L$ was used as a probe in overlay assays of proteins from brain cytosol (Figure 5B) and of recombinantly expressed DPF/W domains of the proposed ligands (Figure 5C). Figure 5B shows that α-ear$_L$ binds directly to proteins of the same apparent molecular weights as amphiphysin, Eps15, epsin, and AP180/clathrin. Figure 5C shows that α-ear$_L$ binds directly to the DPF/W domains of these proteins and to that of auxilin, and that the interaction is lost when the DPF domain is deleted. Thus, AP180 and auxilin can now be considered direct binding partners of α-adaptin appendage domain.

In order to establish that binding requires the DPF/W motif, peptides from amphiphysin (LDLDFDPFKPDV, the DPF peptide) and from epsin (SDPWGSDPWG, the DPW peptide) were used in competition assays alongside the α-adaptin interaction domains of Eps15 and epsin (Benmerah et al., 1996; Chen et al., 1998) for binding to α-adaptin appendage domain from brain cytosol. Both

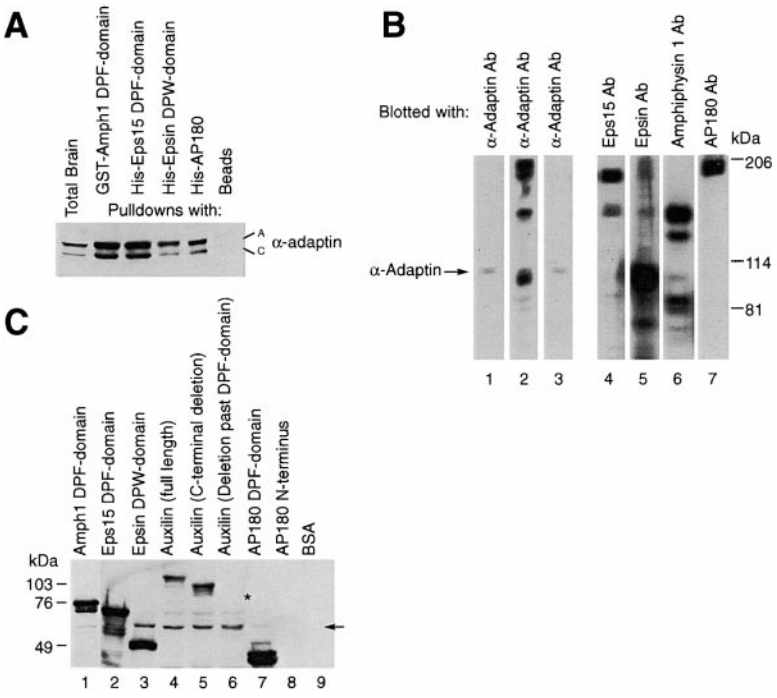

Figure 5. Direct Interaction of α-Adaptin Appendage Domain with Amphiphysin, Eps15, Epsin, AP180, and Auxilin

(A) Immunoblot using an antibody directed against α-adaptin, showing that α-adaptin is "pulled down" from brain cytosol using the DPF/W domains of amphiphysin, Eps15, epsin, and full-length AP180.

(B) Proteins from brain cytosol were separated by SDS–PAGE and then blotted onto nitrocellulose. Lane 1 was overlayed with GST-Grb2, lane 2 with GST-α-ear$_L$, and lane 3 with the W840A mutant of α-ear$_L$. These were then immunoblotted with Ra5.2. Four main proteins are seen to bind to wild-type GST-α-ear$_L$ that have apparent molecular weights corresponding to Eps15, epsin, amphiphysin, and AP180/clathrin, as indicated by immunoblotting lanes 4–7 with antibodies to the respective whole proteins. The W840A mutant binds to nothing.

(C) The proteins indicated were run on SDS–PAGE, blotted onto nitrocellulose, and then overlayed with α-ear$_L$, the presence of which was detected by immunoblotting with Ra5.2. The DPF/W domains of amphiphysin (lane 1), Eps15 (lane 2), and epsin (lane 3) bind to GST α-ear$_L$. Full-length (lane 4) and C-terminally truncated auxilin (lane 5) bind to α-adaptin appendage domain, but truncation beyond the DPF sequences abolishes this interaction (lane 6, where protein runs at the position indicated by the asterisk). AP180 DPF domain binds to α-ear$_L$ (lane 7), whereas the N-terminal domain does not (lane 8). BSA (4 μg) is also included as an additional control. The arrow indicates a contaminating protein present in all pull downs to varying extents. The overlay experiment was repeated with the W840A mutant of α-ear$_L$, and this did not bind specifically to any of the ligands.

peptides at concentrations of 500 μM, but not a control peptide at 2 mM, and both domains strongly inhibit the binding of all the tested ligands to the appendage domain (Figures 6A and 6B). The Coomassie-stained gel (Figure 6A, top panel) shows that all ligands discussed are effectively competed by the epsin DPW domain and the Eps15 DPF domain. Confirmation of the location of the binding site on the appendage domain and of the direct involvement of the DPF/W in the interaction was obtained by following the effect of the addition of the DPF peptide on the intrinsic fluorescence of the only tryptophan residue in the domain, W840, which is situated at the base of the binding pocket. When peptide was added, the fluorescence of the tryptophan was quenched by 17% in a saturable manner, giving a K_D of 117 ± 15 μM (Figure 6C). The mutants E907A and F837A, which showed greatly reduced binding of amphiphysin (see Figure 3) without a change in tertiary structure (as determined by their identical CD and tryptophan excitation and emission spectra), showed no such effects over the range of peptide concentrations used.

Dynamin is implicated in the final stages of clathrin-coated vesicle formation. It interacts with amphiphysin (David et al., 1996; Wigge et al., 1997a), which in turn binds to the appendage domain of α-adaptin. A direct interaction of dynamin with the α-adaptin appendage domain has also been suggested (Wang et al., 1995). To investigate the nature of the interaction in brain cytosol, two peptides were used in competition experiments: peptide P4 (QVPSRPNRAP), which disrupts the amphiphysin–dynamin interaction (see Owen et al., 1998 and Figure 6D,i) and the DPW peptide (SDPWGSDPWG), which disrupts direct interactions with the appendage domain (Figure 6B), but not of dynamin with amphiphysin (Figure 6D,i). P4 displaced bound dynamin from amphiphysin and from the appendage domain, without significantly affecting the binding of amphiphysin to the appendage domain, while the DPW peptide competed off both simultaneously (Figure 6D, ii). Thus, the dynamin interaction with the appendage domain is largely indirect. A small amount of direct binding of dynamin to α-adaptin appendage domain was observed in α-ear$_L$ overlay assays (data not shown, see also Wang et al., 1995), which may be due to the presence of a single DPF sequence in its proline-rich domain (residues 824–826). Thus, the interaction of dynamin with the α-adaptin appendage domain is mainly indirect via amphiphysin, which is in agreement with the proposed role for amphiphysin in the recruitment of dynamin to sites of endocytosis (for review, see Wigge and McMahon, 1998).

Discussion

Clathrin adaptors serve at least three functions. They bind to proteins destined for internalization mainly via their μ subunits. They bind to clathrin triskelia via their β subunits, promoting formation of clathrin cages. In this work, we investigate a third function: the recruitment of proteins via the α-adaptin appendage domain. This domain has been reported to have no effect on clathrin lattice formation and invagination (Peeler et al., 1993); however, the demonstration in this work that the appendage domain of α-adaptin can block clathrin-mediated endocytosis argues against this.

The appendage domain of α-adaptin has a bilobal structure. We have identified a single pocket to which

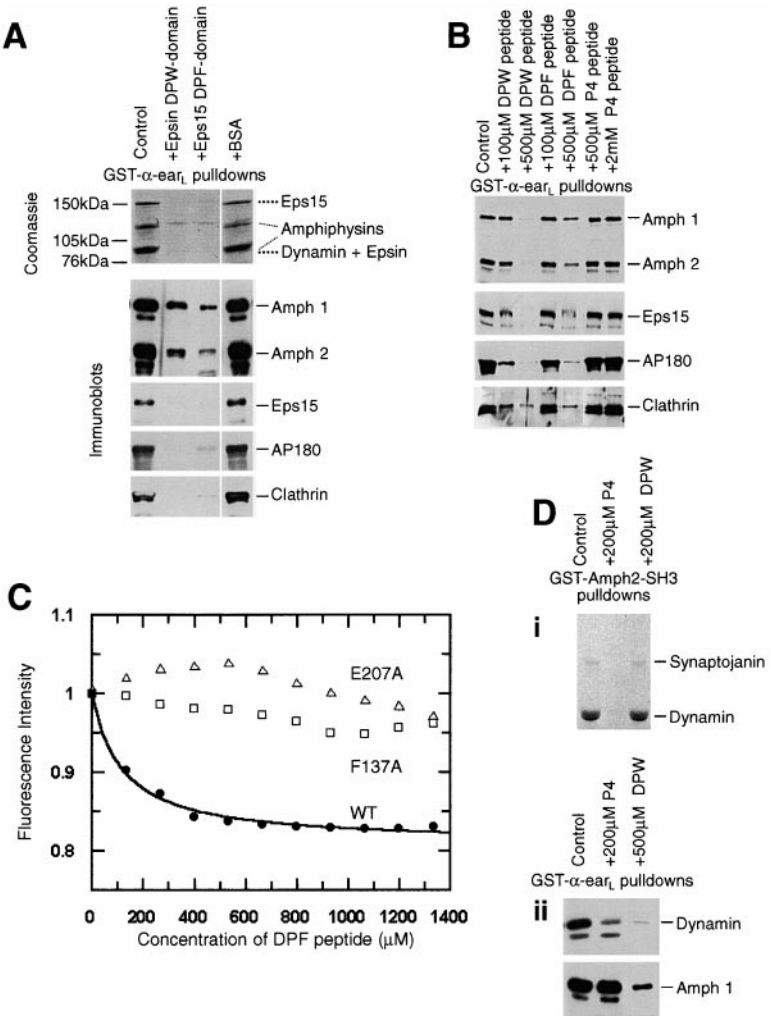

Figure 6. Analysis of α-Adaptin Appendage Domain Ligand Binding

(A and B) Epsin DPW domain and Eps15 DPF domains detected both by Coomassie blue staining (A, upper panel) and by immunoblotting (A, lower panels), and DPW and DPF peptides at concentrations of 500 μM (B) inhibit binding of amphiphysin, Eps15, AP180, and clathrin to GST α-adaptin appendage domain in pull-down experiments from total brain cytosol.

(C) Addition of DPF peptide (125 μM aliquots) to α-adaptin appendage domain causes the intrinsic fluorescence of the only tryptophan residue in the domain, W840, to be quenched by 17% in a peptide concentration-dependent and saturable manner giving a K_D for the interaction of 117 ± 15 μM. The fluorescence of the same residue in the fully folded mutants E907A and F837A, which show greatly reduced binding to amphiphysin (see Figure 3), is not significantly reduced by the addition of peptide over the same concentration range.

(D) (i) The binding of dynamin and synaptojanin to the GST-SH3 domain of amphiphysin in total brain extract is inhibited by P4 peptide but not the DPW peptide.

(ii) Dynamin binds to α-adaptin appendage domain predominantly via amphiphysin. The P4 peptide greatly reduces the amount of dynamin but not amphiphysin detectable in a pull-down experiment with GST-α-adaptin appendage. The DPW peptide greatly reduces the amount of both proteins pulled down.

various proteins implicated in endocytosis (including the amphiphysins, Eps15, epsin, AP180, and auxilin) bind in the C-terminal subdomain. The site is centered at a tryptophan and is surrounded by mainly charged residues. These residues are conserved from mammals to *Drosophila* and between α-adaptin A and α-adaptin C (Robinson, 1989). Mutations in these residues, while not significantly affecting the structure of the appendage domain, are shown to have varying effects on the binding of target proteins, from total abolition (W940, R920) to no significant reduction (E849). The N-terminal β sandwich domain has no apparent binding partners and may thus function as a scaffolding domain or spacer, allowing the C-terminal domain to be displayed in the correct manner.

The only common feature between the regions of amphiphysin 1, Eps15, epsin, AP180, and auxilin, which we show bind directly to the appendage domain of α-adaptin, is that they contain either DPF or DPW motifs. The affinity of binding to α-adaptin appears to be correlated with the number of DPF/W motifs, in that Eps15 and epsin, which contain many copies of this motif, bind more tightly than amphiphysin, AP180, and auxilin, which contain fewer copies. That DPF/W is a major determinant for binding of these domains to α-adaptin appendage domain is also confirmed by the peptide competition and fluorescence data presented. It is interesting to note that AP180 contains 11 copies of the sequence D × F (where × is A, L, or I) in addition to its two DPF sequences in the same region of the protein (for review, see McMahon, 1999). Also amphiphysin 1 has a DNF close to its single DPF, and these could also be involved in binding to this site on the α-adaptin appendage domain.

Eps15 contains three EH domains at its N terminus. The structure of the second EH domain of Eps15 has been solved and bears no structural homology to the C-terminal subdomain of the α-adaptin appendage domain. However, several parallels can be drawn between the binding sites. The EH domain recognizes the motif NPF with a K_D of approximately 500 μM (de Beer et al., 1998), and the α-adaptin domain recognizes DPF in the same range (estimated from peptide fluorescence data). Both binding sites are shallow hydrophobic pockets of similar size (for EH domain structure, see de Beer et al., 1998) that have a tryptophan at the base, and mutation of this W to A abolishes interaction with its binding partners. In both, the tryptophan is surrounded by polar residues, which could provide specificity for their binding targets as a result of complementary electrostatic

Table 2. Statistics on Data Collection and Phasing

	Native	EMTS1	EMTS2
Data Collection[a]			
Resolution (Å) (outer bin)	16–1.9 (2.0)	20–2.82 (2.92)	29–2.2 (2.3)
R_{merge}[b]	0.071 (0.235)	0.085 (0.156)	0.165 (0.256)
R_{meas}[c]	0.088 (0.295)	0.120 (0.221)	0.226 (0.362)
$<<I>/\sigma(<I>)>$	11.5 (5.3)	7.9 (3.5)	5.8 (3.0)
Completeness (%)	96.9 (96.9)	86.4 (90.3)	84.3 (74.5)
Multiplicity	2.8 (2.6)	2.2 (1.9)	2.4 (1.3)
Wilson plot B ($Å^2$)	22	47	47
MIR Phasing			
No. of sites		6	6
R_{deriv}[d]		0.282	0.278
R_{cullis}[e]		0.48	0.48
Phasing power: isomorphous (anomalous)[f]		3.8 (1.3)	3.5 (1.6)
Mean figure of merit	0.307		
Figure of merit after solvent flattening (all data)	0.939		
Refinement			
R (R_{free})[g]		0.169 (0.223)	
$<B>$ ($Å^2$)		20	
No. of reflections (No. in R_{free})		18,198 (1,444)	
No. of atoms (No. of water atoms)		2,192 (298)	
Rmsd bond length (Å)		0.013	
Rmsd angle distance (Å)		0.032	
No. of Ramachandran violations		0	

[a] Values in brackets apply to the high-resolution shell.
[b] $R_{merge} = \Sigma\Sigma_i|I_h - I_{hi}|/\Sigma\Sigma_i I_h$, where I_h is the mean intensity for reflection h.
[c] $R_{meas} = \Sigma\sqrt{(n/n-1)}\Sigma_i|I_h - I_{hi}|/\Sigma\Sigma_i I_h$, the multiplicity weighted R_{merge} (Diederichs and Karplus, 1997).
[d] $R_{deriv} = \Sigma|F_{PH} - F_P|/\Sigma F_P$.
[e] $R_{cullis} = \Sigma||F_{PH} - F_P| - |F_{Hcalc}||/\Sigma|F_{PH} - F_P|$.
[f] Phasing power = $<|F_{Hcalc}|/$phase-integrated lack of closure$>$.
[g] $R = \Sigma|F_P - F_{calc}|/\Sigma F_P$.

interactions (for example McCoy et al., 1997). In the case of the DPF-binding α-adaptin subdomain, there are two arginine residues (R905 and R920), and mutation of the latter also abrogates target protein binding.

The recognition of the DPF/W motif by the α-adaptin appendage domain is another example of a relatively low-affinity protein–protein interaction in endocytosis in which a domain recognizes a short sequence motif. Other such interactions include clathrin heavy chain recognizing LL(D/E/N)ø(D/E) in β-arrestin, amphiphysin and the hinge regions of β-adaptins (where ø is a hydrophobic residue) (Dell'Angelica et al., 1997), AP2 adaptors recognizing Yxxø or (D/E)xxxLL motifs on receptors (Ohno et al., 1995), the SH3 domains of the amphiphysins recognizing PxRPxR (Owen et al., 1998), and EH domains recognizing NPF motifs (de Beer et al., 1998). High on and off rates resulting from such a mode of protein recognition produce a dynamic system that allows rapid exchange of binding partners, and varying the number of copies of a motif can result in differential strengths of binding.

This study maps a single binding site for all the α-adaptin appendage domain ligands. The interaction with this site is predominantly through DPF/W sequences, the number of which present in a ligand is correlated with its affinity for the appendage domain. This is consistent with a model in which α-adaptin binds a series of ligands sequentially throughout the process of endocytosis or binds different ligands in different regions of the nascent vesicle. That Eps15 has a higher affinity for the α-adaptin appendage domain than amphiphysin or AP180 is consistent with the observation that Eps15 is constitutively bound to AP2 complexes when isolated from brain extract (Benmerah et al., 1996), which is displaced from AP2 adaptors on clathrin cage formation. Our study identifies single point mutations in the α-adaptin appendage domain that block endocytosis and may allow the dissection of the steps of coated pit formation when they are incorporated into whole α-adaptin and expressed in eukaryotic cells.

The appendage domain of α-adaptin may therefore serve to coordinate spatially and temporally the recruitment of components of the endocytotic machinery and consequently play a pivotal role in the formation of clathrin-coated vesicles.

Experimental Procedures

Constructs and Protein Expression

The cDNA encoding residues 701–938 of mouse α-adaptin C (the appendage domain) was cloned into the vector pGEX 4T2 for production as an N-terminal GST fusion protein and into pCMV-MYC for eukaryotic expression as an N-terminal Myc tag fusion protein under the control of a CMV promoter. The resulting protein termed α-ear_S was used for structure determination but was insoluble in fibroblasts.

The larger construct α-ear_L (residues 695–983) was cloned in a similar manner, which resulted in production of soluble protein in both systems. Mutants of α-ear_L were made by PCR using primers incorporating the changed bases. The parent plasmid was digested

by Dpn1, and the PCR mixture was transformed into DH5α to amplify the mutated plasmid (Vallis et al., 1999).

GST-fusion protein was expressed in DH5α at 25°C overnight, following induction with 0.2 mM IPTG. The cells were lysed by repeated passage through a French pressure cell, and insoluble material was removed by centrifugation. The cell lysate was loaded on a glutathione-Sepharose column and washed thoroughly with buffer A (0.2 M NaCl, 20 mM HEPES [pH 7.5], 4 mM DTT) and then eluted with buffer A containing 10 mM glutathione. The fusion protein typically expressed at 10 mg/l of culture. For CD, α-adaptin appendage domains were cleaved from its GST fusion protein with bovine thrombin (Sigma) and then dialyzed into 150 mM NaCl, 2 mM HEPES (pH 7.5).

The DPW domain of rat Epsin (residues 249–401), the DPF C-terminal domain of rat Eps15 (residues 529–894), and full-length rat AP180 were cloned into pET15b (Novagen), giving an N-terminal His_6 tag on the proteins when expressed in the bacterial strain BL21 (DE3). The protein was purified from lysed bacteria on a Ni-NTA-agarose column (Qiagen), and bound protein was eluted with buffer A containing 0.3 M imidazole and dialyzed into buffer A. Other constructs were cloned into pGEX4T2 for production as N-terminal GST fusion proteins. These were AP180 N-terminal domain (residues 1–305) and DPF domain (residues 395–482) and full-length bovine auxilin (residues 1–910), C-terminal truncation (1–736), and DPF domain deletion (residues 1–576).

Crystallization and Structure Determination

α-ear_S protein was expressed as a GST fusion, purified from bacteria, and then cleaved by a 16 hr incubation at 30°C with bovine thrombin (Sigma). α-ear_S was then further purified by passage over glutathione-Sepharose followed by fast flow Q Sepharose and finally S200 gel filtration. The protein was dialyzed into 5 mM HEPES, 50 mM NaCl, 4 mM DTT and concentrated to 12 mg/ml giving a final yield of 0.4 mg purified protein per liter of culture.

Crystals were grown by hanging drop vapor diffusion against a reservoir containing 20% PEG 4000, 10% isopropanol, 100 mM sodium citrate (pH 6.0), 10 mM DTT. Crystals (space group P1, unit cell dimensions a = 39.9 Å, b = 40.9 Å, c = 42.5 Å, $\alpha = 99.4°$, $\beta = 95.3°$, $\gamma = 113.7°$) were obtained over period of a week with final dimensions 0.1 × 0.1 × 0.02 mm. Crystals were transferred to 22% PEG 4000, 10% isopropanol, 100 mM sodium citrate (pH 6.0), 10 mM DTT, 15% glycerol, and X-ray diffraction data were collected at 100 K at Elettra (Trieste, native) or on a rotating anode (derivatives) (Table 2). A single mercury derivative was made by soaking a crystal in cryoprotected buffer containing 1 mM ethylmercury thiosalicylate (EMTS) for 2 hr; two different EMTS crystals were used. Data were recorded on a MAR Research image plate, integrated with MOSFLM (Leslie, 1992), and scaled using CCP4 programs (Collaborative Computational Project Number 4, 1994). Mercury sites were determined from difference Pattersons, and heavy-atom refinement and phasing were performed with SHARP (de la Fortelle and Bricogne, 1997), followed by solvent flipping and flattening with SOLOMON (Abrahams and Leslie, 1996), leading to an excellent electron density map at 1.9 Å resolution. The model was built with O (Jones et al., 1991) and refined with REFMAC (Murshudov et al., 1997). The final model consists of residues 702–938 plus 302 water molecules.

Attempts to cocrystallize the protein with DPF/DPW peptides were unsuccessful, probably due to the low affinity of the interaction. The packing of the molecules in the crystal precluded peptide incorporation by soaking, as the binding site was at a crystal interface.

Surface Mapping

The molecular surface of the ear domain was calculated using the MSP suite of programs (Connolly, 1985), with a surfacing probe radius of 1.6 Å. This suite produces a description of the surface in terms of tessellated triangles. Associated with each vertex of each triangle are coordinates of the corresponding position of the surfacing probe. These positions represent the sites that an atom would occupy when in contact with the protein's molecular surface. The hydrophobic interaction potential for these sites was evaluated using the program GRID (Goodford, 1996). The resulting potentials were used to color the protein surface, which was displayed using the program Aesop (M. Noble, unpublished data).

Protein–Protein Binding Assays

Binding assays were performed by incubating 20 μg GST fusion protein with 0.5 ml of 0.1% TritonX-100 brain extract (Owen et al., 1998) in buffer A in the presence of 20 μl 50% slurry of glutathione-Sepharose at 4°C for 1 hr. The beads were washed three times for 5 min with buffer A, and the proteins bound were analyzed by SDS–PAGE and immunoblotting. Polyclonal rabbit antibodies used were as follows: Ra3 (anti-Amphiphysin 1), Ra1.2 (anti-Amphiphysin 2), Ra5.2 (anti α-adaptin appendage domain), D632 (anti-Dynamin, kind gift of T Südhof), Ra14 (anti-Epsin), Ab131 (anti-Synaptojanin, kind gift of P. Parker), and A14 (anti-Myc, from Santa Cruz). Monoclonal antibodies used were anti-AP180 (Sigma), anti-Clathrin Heavy Chain (Transduction), anti-α-adaptin (Transduction), and anti-Auxilin (kind gift of E. Ungewickell).

Fluorescence

Fluorescence measurements were made using a Perkin Elmer LS 50B spectrofluorimeter. Protein fluorescence of wild-type and mutant α-adaptin appendage domains were measured using an excitation wavelength of 280 nm and detecting at 340 nm. Slit widths of 2.5 nm and 4.0 nm were used for the excitation and emission beams, respectively. Experiments took place in a 500 μl cuvette with a path length of 1 cm on the excitation axis and 0.2 cm on the emission axis. DPF peptide (LDLDFDPFKPDV) was added in 125 μM aliquots, and each titration was performed with an initial protein concentration of 13.5 μM. The results are the average of three experiments. Dilution effects caused by the addition of peptide were corrected for, and the data, where possible, were fitted to a weak binding hyperbola of $F = Fo - (L \cdot Po)/(K_D + L)$, where F is the fluorescence intensity, Fo is the fluorescence intensity with no ligand, L is the ligand concentration, K_D is the binding constant, and Po the initial protein concentration.

Protein Overlay Assay

Brain extract or expressed proteins (1 μg/lane) were separated on SDS–PAGE and transferred onto nitrocellulose. After blocking with 5% milk, the blots were incubated overnight with 1 μg/ml α-ear_L in 10% goat serum. After washing extensively, bound α-adaptin appendage domain was detected with an antibody raised against the domain (Ra5.2).

Endocytosis Assay and Immunocytochemistry

Clathrin-mediated endocytosis was measured by assaying transferrin uptake into COS-7 fibroblasts. Forty-eight hours posttransfection cells were incubated at 37°C in serum-free DMEM for 1 hr, and then at 37°C in DMEM containing 25 μg/ml biotinylated human transferrin (Sigma) for 30 min (Wigge et al., 1997b). Transferrin uptake was visualized with FITC-conjugated streptavidin (seen as a punctate green perinuclear staining), and the Myc-tagged proteins were visualized using the polyclonal antibody A14 (Santa Cruz Labs) followed by Texas red–conjugated anti-rabbit antibody (Chemicon). Cells were imaged on an MRC 1024 scanning confocal microscope, and transfected cells were compared with untransfected cells in the immediate vicinity. For quantitation "blocked cells" were defined as all transfected cells in which transferrin uptake was <20% of normal. Blocked cells were then expressed as a percentage of the total number of transfected cells in multiple fields (see Figure 4).

Acknowledgments

We would like to thank Eric de la Fortelle for assistance with SHARP, Franco Zanini and the staff at Elettra for assistance with data collection, Molly Craxton for computer searches, Margaret Robinson for the α-adaptin clone and helpful comments, Ernst Ungewickell for reagents, Patrick Wigge for extensive discussion, and all who have kindly shared their antibodies as listed in Experimental Procedures.

Received February 10, 1999; revised May 12, 1999.

References

Abrahams, J.P., and Leslie, A.G.W. (1996). Methods used in the structure determination of bovine mitochondrial F1 ATPase. Acta Crystallogr. D *52*, 30–42.

Ahle, S., and Ungewickell, E. (1986). Purification and properties of a new clathrin assembly protein. EMBO J. *5*, 3143–3149.

Anderson, R.G. (1998). The caveolar membrane system. Annu. Rev. Biochem. *68*, 199–225.

Benmerah, A., Gagnon, J., Begue, B., Megarbane, B., Dautry-Varsat, A., and Cerf-Bensussan, N. (1995). The tyrosine kinase substrate eps15 is constitutively associated with the plasma membrane adaptor AP-2. J. Cell Biol. *131*, 1831–1838.

Benmerah, A., Begue, B., Dautry-Varsat, A., and Cerf-Bensussan, N. (1996). The ear domain of alpha-adaptin interacts with the COOH-terminal domain of the Eps15 protein. J. Biol. Chem. *271*, 12111–12116.

Carbone, R., Fre, S., Iannolo, G., Belleudi, F., Mancini, P., Pelicci, P.G., Torrisi, M.R., and Di Fiore, P.P. (1997). Eps15 and Eps15R are essential components of the endocytic pathway. Cancer Res. *57*, 5498–5504.

Chen, H., Fre, S., Slepnev, V.I., Capua, M.R., Takei, K., Butler, M.H., Fiore, P.P.D., and Camilli, P.D. (1998). Epsin is an EH-domain-binding protein implicated in clathrin-mediated endocytosis. Nature *394*, 793–797.

Collaborative Computational Project, Number 4 (1994). The CCP4 suite: programs for protein crystallography. Acta Crystallogr. D *50*, 760–763.

Connolly, M. (1985). Molecular surface triangulation. J. Appl. Crystallogr. *18*, 499–505.

David, C., McPherson, P.S., Mundigl, O., and DeCamilli, P. (1996). A role of amphiphysin in synaptic vesicle endocytosis suggested by its binding to dynamin in nerve terminals. Proc. Natl. Acad. Sci. USA *93*, 331–335.

de Beer, T., Carter, R.E., Lobel-Rice, K.E., Sorkin, A., and Overduin, M. (1998). Structure and Asn-Pro-Phe binding pocket of the Eps15 homology domain. Science *281*, 1357–1360.

DeCamilli, P., and Takei, K. (1996). Molecular mechanisms in synaptic vesicle endocytosis and recycling. Neuron *16*, 481–486.

de la Fortelle, E., and Bricogne, G. (1997). Maximum-likelihood heavy-atom parameter refinement for multiple isomorphous replacement and multiwavelength anomalous diffraction methods. Methods Enzymol. *277*, 472–494.

Dell'Angelica, E.C., Ohno, H., Ooi, C.E., Rabinovich, E., Roche, K.W., and Bonifacino, J.S. (1997). AP-3: an adaptor-like protein complex with ubiquitous expression. EMBO J. *16*, 917–928.

DeTulleo, L., and Kirchhausen, T. (1998). The clathrin endocytic pathway in viral infection. EMBO J. *17*, 4585–4593.

Diederichs, K., and Karplus, P.A. (1997). Improved R-factors for diffraction data analysis in macromolecular crystallography. Nat. Struct. Biol. *4*, 269–275.

Floyd, S., and DeCamilli, P. (1998). Endocytosis proteins and cancer: a potential link? Trends Cell Biol. *8*, 299–301.

Gallusser, A., and Kirchhausen, T. (1993). The B1 and B2 subunits of the AP complexes are the clathrin coat assembly components. EMBO J. *12*, 5237–5244.

Goodford, P. (1996). Multivariate characterisation of molecules for QSAR. J. Chemometrics *10*, 107–117.

Heuser, J.E., and Keen, J. (1988). Deep-etch visualisation of proteins involved in clathrin assembly. J. Cell Biol. *107*, 877–886.

Iannolo, G., Salcini, A.E., Gaidarov, I., Goodman, O.B., Baulida, J., and Carpenter (1997). Mapping of the molecular determinants involved in the interaction between Eps15 and AP-2. Cancer Res. *57*, 240–245.

Jones, T.A., Zou, J.Y., Cowan, S.W., and Kjeldgaard, M. (1991). Improved methods for building protein models in electron density maps and the location of errors in these models. Acta Crystallogr. A *47*, 110–119.

Keen, J.H. (1987). Clathrin assembly proteins: affinity purification and a model for coat assembly. J. Cell Biol. *105*, 1989–1998.

Kreis, T.E., Lowe, M., and Pepperkok, R. (1995). COPs regulating membrane traffic. Annu. Rev. Cell Dev. Biol. *11*, 677–706.

Leslie, A.G.W. (1992). Recent changes to the MOSFLM package for processing film and image plate data. In Joint CCP4 and ESF-EACMB Newsletter on Protein Crystallography No. 26. (Warrington, UK: Daresbury Laboratory).

Lindner, R., and Ungewickell, E. (1992). Clathrin-associated proteins of bovine brain coated vesicles. An analysis of their number and assembly-promoting activity. J. Biol. Chem. *267*, 16567–16573.

McCoy, A.J., Epa, Y.C., and Colman, P.M. (1997). Electrostatic complementarity at protein-protein interfaces. J. Mol. Biol. *268*, 570–584.

McMahon, H.T. (1999). Endocytosis: an assembly protein for clathrin cages. Curr. Biol. *9*, R332–R335.

Murshudov, G.N., Vagin, A.A., and Dodson, E.J. (1997). Refinement of macromolecular structures by the maximum-likelihood method. Acta Crystallogr. D *53*, 240–255.

Odorizzi, G., Cowles, C.R., and Emr, S.D. (1998). The AP-3 complex: a coat of many colours. Trends Cell Biol. *8*, 282–288.

Ohno, H., Stewart, J., Fournier, M.C., Bosshart, H., Rhee, I., Miyatake, S., Saito, T., Gallusser, A., Kirchhausen, T., and Bonifacino, J.S. (1995). Interaction of tyrosine-based sorting signals with clathrin-associated proteins. Science *269*, 1872–1875.

Oldridge, J., and Marsh, M. (1998). Nef—an adaptor adaptor? Trends Cell Biol. *8*, 302–305.

Owen, D.J., and Evans, P.R. (1998). A structural explanation for the recognition of tyrosine-based endocytotic signals. Science *282*, 1327–1332.

Owen, D.J., Wigge, P., Vallis, Y., Moore, J.D.A., Evans, P.R., and McMahon, H.T. (1998). Crystal structure of the Amphiphysin-2 SH3 domain and its role in prevention of dynamin ring formation. EMBO J. *17*, 5273–5285.

Pearse, B.M. (1976). Clathrin: a unique protein associated with intracellular transfer of membrane by coated vesicles. Proc. Natl. Acad. Sci. USA *73*, 1255–1259.

Pearse, B.M.F., and Robinson, M.S. (1990). Clathrin, adaptors and sorting. Annu. Rev. Cell Biol. *6*, 151–171.

Peeler, J.S., Donzell, W.C., and Anderson, R.G.W. (1993). The appendage domain of the AP2 subunit is not required for assembly or invagination of clathrin-coated pits. J. Cell Biol. *120*, 47–54.

Robinson, M.S. (1989). Cloning of cDNAs encoding two related 100kD coated vesicle proteins (α-adaptins). J. Cell Biol. *108*, 833–842.

Robinson, M.S. (1997). Coats and vesicle budding. Trends Cell Biol. *7*, 99–102.

Roth, T.F., and Porter, K.R. (1964). Yolk protein uptake in the oocyte of the mosquito aedes aegypti L. J. Cell Biol. *20*, 313–332.

Schekman, R., and Orci, L. (1996). Coat proteins and vesicle budding. Science *271*, 1526–1533.

Schmid, S.L. (1997). Clathrin-coated vesicle formation and protein sorting: an integrated process. Annu. Rev. Biochem. *66*, 511–548.

Schmid, S.L., McNiven, M.A., and De Camilli, P. (1998). Dynamin and its partners: a progress report. Curr. Opin. Cell Biol. *10*, 504–512.

Shih, W., Gallusser, A., and Kirchhausen, T. (1995). A clathrin-binding site in the hinge of the beta 2 chain of mammalian AP-2 complexes. J. Biol. Chem. *270*, 31083–31090.

Slepnev, V.I., Ochoa, G.C., Butler, M.H., Grabs, D., and Camilli, P.D. (1998). Role of phosphorylation in regulation of the assembly of endocytic coat complexes. Science *281*, 821–824.

Smith, C.J., Grigorieff, N., and Pearse, B.M. (1998). Clathrin coats at 21 Å resolution: a cellular assembly designed to recycle multiple membrane receptors. EMBO J. *17*, 4943–4953.

Swanson, J.A., and Watts, C. (1995). Macropinocytosis. Trends Cell Biol. *5*, 424–428.

Tebar, F., Sorkina, T., Sorkin, A., Ericsson, M., and Kirchhausen, T. (1996). Eps15 is a component of clathrin-coated pits and vesicles and is located at the rim of coated pits. J. Biol. Chem. *271*, 28727–28730.

Vallis, Y., Wigge, P., Marks, B., Evans, P.R., and McMahon, H.T. (1999). Importance of the pleckstrin homology domain of dynamin in clathrin-mediated endocytosis. Curr. Biol. *9*, 257–260.

Wang, L.-H., Südhof, T.C., and Anderson, R.G.W. (1995). The appendage domain of α-adaptin is a high affinity binding site for dynamin. J. Biol. Chem. *270*, 10079–10083.

Wigge, P., and McMahon, H.T. (1998). The amphiphysin family of proteins and their role in endocytosis at the synapse. Trends Neurosci. *21*, 339–344.

Wigge, P., Kohler, K., Vallis, Y., Doyle, C.A., Owen, D., Hunt, S.P., and McMahon, H.T. (1997a). Amphiphysin heterodimers: potential role in clathrin-mediated endocytosis. Mol. Biol. Cell *8*, 2003–2015.

Wigge, P., Vallis, Y., and McMahon, H.T. (1997b). Inhibition of receptor-mediated endocytosis by the amphiphysin SH3 domain. Curr. Biol. *7*, 554–560.

Ye, W., and Lafer, E.M. (1995). Bacterially expressed F1–20/AP3 assembles clathrin into cages with a narrow size distribution: implications for the regulation of quantal size during neurotransmission. J. Neurosci. Res. *41*, 15–26.

Zaremba, S., and Keen, J.H. (1985). Limited proteolytic digestion of coated vesicle assembly polypeptides abolishes reassembly activity. J. Cell Biochem. *28*, 47–58.

Zhang, B., Koh, Y.H., Beckstead, R.B., Budnik, V., Ganetzky, B., and Bellen, H.J. (1998). Synaptic vesicle size and number are regulated by a clathrin adaptor protein required for endocytosis. Neuron *21*, 1465–1475.

Protein Data Bank ID Code

The coordinates and structure factors have been deposited with the ID code 1b9k.